Final Draft

of the original manuscript

Yang, H.; Patel, J.; Yang, X.; Gavras, S.; Dieringa, H.:

Properties of Mg-based Metal Matrix Nanocomposites Processed by High Shear Dispersion Technique (HSDT) - A Review.

In: Current Nanomaterials. Vol. 6 (2021) 2, 106 - 118.

First published online by Bentham Science: 06.07.2021

https://dx.doi.org/10.2174/2405461506666210420133620

Properties of Mg-based Metal Matrix Nanocomposites Processed by High Shear Dispersion Technique (HSDT) - A Review

Hong Yang[1,2], Jayesh B. Patel[3], Xinliang Yang[4], Sarkis Gavras[5,6] and Hajo Dieringa[5,7,*]

[1]State Key Laboratory of Mechanical Transmissions, College of Materials Science and Engineering, Chongqing University, Chongqing, 400044, China; [2]National Engineering Research Center for Magnesium Alloys, Chongqing University, Chongqing, 400044, China; [3]BCAST, Brunel University London, Uxbridge, UB8 3PH, UK; [4]WMG (Warwick Manufacturing Group), The University of Warwick, Coventry, CV4 7AL, UK; [5]Helmholtz-Zentrum Hereon, MagIC-Magnesium Innovation Centre, Max-Planck-Str. 1, 21502 Geesthacht, Germany; [6]Helmholtz-Zentrum Hereon, Institute of Metallic Biomaterials, Max-Planck-Str. 1, 21502 Geesthacht, Germany; [7]Helmholtz-Zentrum Hereon, Institute of Materials and Process Design, Max-Planck-Str. 1, 21502 Geesthacht, Germany

Abstract: Metal Matrix Nanocomposites (MMNCs) often show excellent properties as compared to their non-reinforced alloys due to either the achieved grain refinement or Orowan strengthening. Especially in light metals such as aluminium and magnesium as the matrix has the potential to be significantly improved in relation to mechanical properties. Functionalisation can also be achieved in some cases. However, the challenge lies in the homogeneous distribution of the ceramic nanoparticles in the melt if MMNCs have been processed *via* melt metallurgical processes. The large surface area of the nanoparticles generates large van der Waals forces, which need to be overcome. Furthermore, the wettability of the particles with molten metal is difficult. Additional forces can be applied by ultrasound, electromagnetic stirring, or even high-shearing. In this paper, properties of MMNCs with a light metal matrix, which have been produced with the High-Shearing Dispersion Technique are discussed. First, the process with its different characteristics and the underlying theory is presented, and then property improvements are discussed by comparing MMNCs to their matrix materials.

Keywords: Magnesium Alloys, nanoparticles, high shear dispersion technique, dispersion, creep, strength.

1. INTRODUCTION

The low density of magnesium alloys has made it a good choice for many years in lightweight metallic materials for the automotive and aviation industries. They combine low weight, very good castability, and also very good machinability. However, the flammability of the melt, moderate corrosion properties and the market dominance of China as the primary producer of the vast majority of magnesium have a negative impact. The mechanical and physical properties of magnesium alloys are excellent but can be improved to only a certain extent by alloying. Magnesium-based composite materials further expand this spectrum. A relatively new type of composites are metal matrix nanocomposites (MMNCs), in which reinforcing phases with a diameter of less than 500 nm in two dimensions are introduced into the magnesium alloy. These can be ceramic particles [1-5], CNTs [6, 7], C-dots, graphene [8, 9] or nanodiamonds [10-12]. It has been shown that strength and ductility could be increased at the same time , and in addition to Orowan strengthening, it is possible to achieve a grain refinement, which also increases strength [6, 13]. MMNCs can be produced using powder metallurgical processes or melt metallurgical ones. Concerning the latter, due to the small size of the particles, their surface area is very large, which leads to large van der Waals forces, resulting in agglomeration of the particles in molten metal. In addition, some of the ceramic or carbon-based phases have poor wettability with molten metal. For these reasons, additional forces must be applied to break up the agglomerates during the melt-metallurgical production of the nanocomposite [14]. This can be done by ultrasonic cavitation [15], electromagnetic stirring [16, 17], or additional shearing when stirring in the particles. Several review articles have already been published on the production, properties and potential applications of magnesium-based metal matrix nanocomposites (Mg-MMNCs) [7, 15-21]. In fields where magnesium alloys are already used, such as aerospace, automotive, medical and consumer electronics, magnesium-based nanocomposites can expand the range of applications. Higher strengths through grain refinement or through Orowan strengthening and ductility enhancement allow use in application fields where only aluminum alloys can be used today. But also the application in civil or military drones seems to be a potential field, as here lightweight construction is very significant because it in-

* Address correspondence to this author at the Helmholtz-Zentrum Hereon, MagIC-Magnesium Innovaton Centre, Max-Planck-Str. 1, 21502 Geesthacht, Germany; Helmholtz-Zentrum Hereon, Institute of Materials and Process Design, Max-Planck-Str. 1, 21502 Geesthacht, Germany;
E-mail: hajo.dieringa@hereon.de

creases the operating range of the drones and, at the same time, the structural reliability.

In this review, magnesium-based nanocomposites and their properties produced by the High Shear Dispersion Technique (HSDT) process will be described.

2. THEORY OF HIGH SHEAR DISPERSION

The industrial prospect of mixing/dispersing was originated from chemical, pharmaceutical and pulp & paper industries to reduce the inhomogeneity of the product with two or more matter components, where the inhomogeneity can be the distribution of concentration, phase or temperature [22]. With the extensive technological development of mixing/dispersing, a large variety of the equipment and facilities has been commercialized and standardised in aspects of shear rate, energy dissipation, mixing time, processing environment and volume capacity. The adaption of the mixing/dispersing technology is conducted to other industries.

Metallurgy, a technique focused on the metal alloying process, has drawn attention on the addition of the foreign components into the metal since the oxide dispersion strengthened (ODS) superalloys in 1970s [23] with significantly enhanced high temperature performance, and then extensive metal matrix composites (MMCs) for aerospace application in late 1980s [24]. Extensive research interest was drawn to the material design through the addition of foreign components (reinforcement) into the matrix materials to achieve superior physical, chemical and mechanical properties. As a mixture of foreign components and metallic materials, the homogeneity of the MMCs are recognised as one of the critical factors to harness the advanced material performance. Thus, the treatment of mixing/dispersing converged into the metallic materials as a foundation of MMCs development.

2.1. The Need for Particle Dispersion in the Metallurgy

The MMCs, with advanced properties, is one of the major material innovations of modern times [24]. The flexible combination of reinforcements, matrix materials and fabrication methods led to a large group of construction/functional composite materials being developed with different physical, chemical and mechanical properties for engineering applications [25]. The reinforcements are generally catalogued into three major types: continuous fibres, short fibres/whiskers and particles. Compared to the fibre/short whiskers reinforced MMCs, the particle reinforcement provides uniform mechanical/physical properties of the composite materials, as they are free from fibre alignment directions to reduce the anisotropy of the material. The particle reinforcement has a wide choice of ceramic particles including oxides, nitrides, carbides, silicates, borides, sulfides, variety of metal and intermetallic particles [26-30]. More recently graphene, carbon nanotubes (CNT) [31, 32] have also become popular. In the pursuit of advanced MMCs properties, the dimensions of the reinforcing particles went from micronscale to the nanoscale. Such material is termed metal matrix nanocomposites.

It is well accepted that, the homogenous distribution of reinforcing particles is a necessity to maximise the performance of particulate reinforced composites [33]. The powder metallurgy was the most commercialized processing method to produce the MMCs with uniform distribution of reinforcement, as the homogeneity of the material was guaranteed through the powder tumble blending and a multi-pass thermal-mechanical process [34]. With the rising expectation of component complexity and material cost-effectiveness [35], the liquid metal processing route has a promising advantage for manufacturing the next generation MMCs. This technological route includes liquid mixing method, semi-solid casting, infiltration, spray deposition [33], and newly merged additive manufacturing [36]. The liquid mixing method shares a dominant volume of the production due to the low facility criteria, high flexibility of the volume capacity and component geometry. However, the reinforcing particle agglomeration, limited wetting of liquid metal on the ceramic particle, and thus consequent porosity defects are major obstacles that prevent the particulate reinforced MMCs from achieving advanced properties [37].

The reinforcing particle agglomeration in the liquid metal is a reflection of the nature of the particle cohesion. Such a phenomenon is caused by the particle surface characteristics, material bridges, and sometimes mechanical locking [38]. The van der Waals force [39] is recognised as the attracting force for the cluster/agglomerate formation in ceramic particles. A more dominant influence is expected with the particle size decreasing from fine ($d<100$ μm), ultrafine ($d<10$ μm) to nano-sized ($d<100$ nm). In some applications, electrostatic forces may be found in the particle addition of electric conductor and non-conductor [40]. Material bridges between the particle surfaces are formed through (i) the liquid bridges due to the low viscous wetting liquid through the capillary pressure and the surface tension, *e.g.* moisture on the particle; and (ii) the solid bridges by crystallization of solvents, solidification of viscous bond agents, contact fusion of the surface impurity, and the solid-state sintering of the reinforcing particles [41, 42].

The wetting of liquid metal to the non-metallic particle is normally poor due to the diversion of their interfacial characteristics, which causes difficulty to incorporate reinforcing particles into the molten metal and alloys, and the deteriorates distribution of reinforcement by the agglomerate/cluster formation. Alloying elements with higher oxygen partial pressure tend to concentrate at the melt surface, which helps to reduce the surface energy and thereby improve the wetting of liquid metal on the ceramic particles. Mg is known to decrease the surface tension of the molten metal due to its low surface tension (0.599 N/m) [43]. With 3 wt.% Mg in the Al melt, the surface tension of the melt reduced from 0.760 N/m to 0.620 N/m [44]. Furthermore, surface modification of reinforcing particles by doping the metallic elements also reduces the surface tension between the reinforcement and the matrix melt. With the Ni or Cu doping [45, 46], the CNTs have successfully been introduced into the Al melt with a high reinforcement yield in the matrix. The improved wetting of the molten matrix to the reinforcement al-

so promotes the liquid metal to penetrate into the gaps between neighbouring particles and reduce the tendency of agglomeration.

Besides the above mentioned factors, interfacial reaction of the reinforcing particles and the interaction between the particle and the solidification front of matrix metal may also influence the MMCs production. The interfacial reaction can cause the particle bridging due to the particle growth under the thermodynamic reaction, which also results in changes to the composition of alloy matrix through the new phase formation and influence the basic properties such as the melting point and strength of the matrix [47]. In the solidification of particulate reinforced MMCs, the interaction between the particle and the solidification front of matrix metal will change the distribution of the reinforcing particles as a result of the development of the solidification microstructure. The majority of reinforcing particles experience the pushing at the solid/liquid interface during the solidification [48]. In commercial alloys, the redistribution of the reinforcement can be influenced by the solidification rate as the reinforcing particles are pushed into the network of inter-dendritic area. The finer network of the inter-dendritic region will result in a more uniform distribution of the reinforcing particles.

2.2. The Dispersion of Reinforcing Particles in the Liquid Metal

As a promising solution to improve the homogeneity of MMCs in the liquid metal mixing process, dispersion of solid powder particles in liquid is of great importance. The enhanced dispersion of reinforcement will substantially affect the physical, chemical and mechanical properties of the resulting products. The object of the dispersion is to break agglomerates to discrete particles and then distribute them uniformly throughout the liquid [38].

The fragmentation theory [49, 50] is commonly used to refer a broader class of processes involving breakup of solid clusters/agglomerates. The two main processes considered in the theory are rupture and erosion [51]. The Fragmentation number (*Fa*) characterizes the breakup due to hydrodynamic forces. It is the ratio between the viscous shear stress and the strength of the agglomerate [52].

$$\boldsymbol{Fa} = \frac{\mu\dot{\gamma}}{\boldsymbol{T}} \tag{1}$$

where γ is the magnitude of the rate-of-deformation tensor which equals to $\sqrt{2D:D}$, *D* equals to $[\nabla_v + (\nabla_v)^T]/2$, where *V* is the velocity of the flow. The term T denotes the characteristic cohesive strength of the agglomerate and plays a role analogous to the surface tension in the definition of the Capillary number of liquid drops [53].

The adhesive strength of agglomerates is a combination of the strength of inter-particle bonds due to van der Waals forces, moisture or electrostatic charges [39, 40]. Several models have been developed to describe the adhesive strength and the simplest model describes two neighbouring particles. Rumpf's model considers the agglomerate as a collection of spherical particles with a radius *a*, occupying a volume fraction ö, bonded to each other *via* cohesive forces. According to this model [54], the tensile strength of agglomerates are given as:

$$\boldsymbol{T} = \frac{9}{32}\frac{\varphi}{\pi a^2}\boldsymbol{n_b F} \tag{2}$$

where *F* is the average binding force of a single bond and nb is the average number of bonds per particle. For the particle size of ~5 µm, the strength of SiC agglomerates could be in the range of 10^2 Pa [55].

Kendall proposed a model assuming that the breakage occurs at a strength limiting flaw, and the expression of the strength of the agglomerate [56] is given as:

$$\boldsymbol{T} = \boldsymbol{11.03}\frac{\varphi^4\Gamma_c^{5/6}\Gamma^{1/6}}{\sqrt{l_f a}} \tag{3}$$

where Γ_c and Γ are the fracture surface energy and the equilibrium surface energy, respectively, and lf is the flaw size. In this model, the influence of the fractal structures in the agglomerate has been considered compared to Rumpf's theory.

The understanding of the cohesive bonding of particles in agglomerates makes it clear that sufficient forces are required to overcome the cohesive forces and break up the agglomerate into discrete particles to achieve a good dispersion of particles in the liquid.

The external forces required for uniform dispersion of the reinforcing particles in the solid-liquid system is provided by the mechanical energy input into the liquid-solid system. In the high shear process, the energy input creates a turbulent flow field in which solid particles are introduced from top/bottom of the vessel and subsequently dispersed and distributed in the liquid. The dispersion of solid particles is achieved by a combination of drag and lift forces of the moving fluid on the solid particles and the bursts of turbulent circulated eddied liquid originating from the bulk flow in the vessel [22], which is illustrated in Fig. (**1**).

The term high shear is normally referred to as the high shear rate generated by the specific dispersion device. By assuming the equal rotor tip velocity, the nominal shear rate γ in the rotor-stator gaps can be calculated [22] as:

$$\dot{\boldsymbol{\gamma}} = \frac{\pi \boldsymbol{ND}}{\boldsymbol{\delta}} \tag{4}$$

where the *N* is the rotational speed of the rotor, *D* is the rotor diameter and *δ* is the gap width between the rotor and stator. By combining the dynamic viscosity of the treated liquid flow *η*, the shear stress *τ* can be estimated as:

$$\boldsymbol{\tau} = \boldsymbol{\eta}\frac{\pi \boldsymbol{ND}}{\boldsymbol{\delta}} \tag{5}$$

This equation is the criteria for the device design to concur the cohesive force of the targeted particle clusters, and lead to a well dispersion of the particles in the liquid flow.

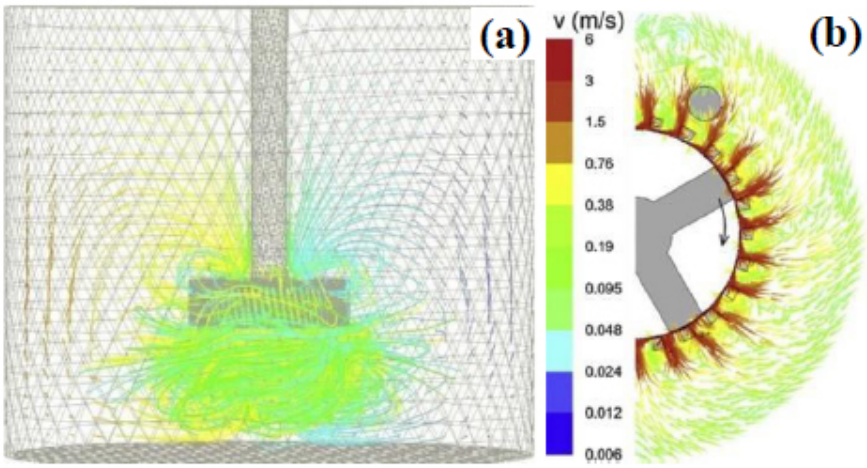

Fig. (1). The simulation of a flow pattern of liquid with rotor-stator mixer processing, (**a**) global view of flow field [57], and (**b**) detailed section of mixing head [58]. *(A higher resolution / colour version of this figure is available in the electronic copy of the article).*

After the mixture of the liquid flow and the particles are delivered into the gap between the rotor and stator, the liquid will be further ejected out through the apertures on the stator head at a high speed. The shear stress will be applied to the particle clusters by the large velocity gradient generated by the boundary layer effect between the inner wall surface of the aperture and the centre of the aperture. This shear phenomenon further breaks-up the agglomerate/-cluster of the reinforcing particles. The shear stress on the mixture of liquid flow and the reinforcing particles flowing through the stator aperture can be calculated [59] as:

$$\tau = f\rho v^2/2 \quad (6)$$

where f is the flow friction factor, ρ is the fluid density of the mixture and v is the mean flow velocity.

From the physical analysis, it is clear that the shear rate is the key device parameter to increase the shear stress for agglomerate/cluster break-up. With the finer particle addition in the liquid flow, the higher shear rate by the increased rotating speed and reduced rotor-stator gap will be needed for the required dispersion effect.

The concept of high shear treatment in Al and Mg melts has been extensively studied and well understood in terms of solidification and application to industrial casting processes to solve some commonly associated fundamental problems. It has also proven to be applicable to different casting processes making it a 'multi-purpose' liquid metal treatment technology, which can be easily integrated to benefit various industrial casting processes.

3. EQUIPMENT FOR HSDT

In the initial times, the primary dispersing means in the MMCs production was the impeller stirring [37], which compile the variety of design of the impeller head and buffers, and the shear rate is in the range of 10^2 s^{-1} to 10^3 s^{-1}. This was useful in the MMCs production with fine particle size. By the increasing understanding of the benefit of composites materials with finer reinforcing particle, more powerful dispersing technologies with higher shear rates and energy dissipation are expected to break-up the agglomerates/-clusters when nano-sized reinforcing particles are introduced into the molten matrix.

3.1. The Material Consideration

Due to the significant difference in the service conditions, the design of high shear devices for chemical engineering cannot be easily transplanted to the scenario of liquid metal treatment. The properties of the suitable material must match the design of the components, but at the same time take into account the harsh environment.

The graphite and the metallic materials with refractory coating are the typical materials for the conventional impellers as the impeller rigidity and the high temperature durability was sufficient under the low shear rate condition [60]. With the increasing shear rate and dynamic fluid flow, the materials with high temperature stiffness, toughness, fatigue and wear resistance, and limited thermal expansion coefficient is desired to build the high shear dispersion device for a chemically harsh and stress complexed environment.

Superior to these desired characteristics of materials, the durability of the device candidate materials in the molten metal is the essential factor determining its engineering practicality for the high shear dispersion device [61]. It is generally accepted the material's life in the molten metal and alloys can be affected by the chemical corrosion and physical erosion. From a systematic study of a variety of the engineering materials under liquid Al, Yan and Fan [62] proposed a selection guidance for high durable materials for high shear dispersion. Here quoted as: "(i) low solubility in liquid metal; (ii) limited thickness and dissolution rate of the interfacial layer; (iii) the interfacial layer should be dense and well

bonded to the substrate; (iv) a high hardness layer is required to protect the substrate from wear and erosion under dynamic condition".

Using an extensive trial and a long period test, a narrowed range of a candidate material is framed for Al and Mg melt treatment. At the current state, the ceramics such as, the silicon carbide, aluminium oxides, boron nitride, silicon nitride, sialon and metallic materials, such as tool steel and NbTiW alloys [63, 64], are shortlisted for molten Al. The nickel-free high temperature steels are the preferred materials for liquid Mg application [65].

3.2. The Type of High Shear Dispersion Equipment

There are two mechanisms of twin-screw and rotor-stator, which were utilised to design and prototype the high shear dispersion devices for liquid Al and Mg which have been produced during the R&D activities in the last two decades [66, 67]. High shear treatment of Al and Mg melts in liquid and semisolid states, using a twin-screw device, was first developed to refine the microstructure and improve the mechanical properties of both cast and wrought alloys [68, 69]. Due to the size of the twin-screw device, the incorporation of this method into the existing processing chain is difficult. Thus, a simpler design to incorporate the high shear treatment into a process is required, leading to the development of a new technology based on a rotor-stator shearing mechanism [64].

3.2.1. Twin-screw Design

Twin-screw mixer is popular in the plastics industry to obtain good mixing of polymer powder/granular with various additives [70]. The main advantages of the twin-screw device are the excellent dispersive mixing of materials with high viscosity, continuous processing and multistage capability.

In 2000, Fan and co-workers developed the prototype of twin-screw device for application to liquid metal for melt conditioning of various melts [71, 72]. The device is constructed with five main sub-systems [65], (i) a driving motor to rotate twin-screws, (ii) the feeder and treatment barrel to host melt flow, (iii) the C shape heating elements embracing treatment barrel and thermocouple to maintain melt temperature, (iv) a pair of co-rotating and intermeshing screws applying high shear to the alloy melt, and (v) a control valve to release the treated melt to down-stream process.

The process starts with the liquid metal fed into the treatment chamber with a pre-set temperature, and then the twin-screws rotate at speed up to 1000 rpm using the driving force from the motor. The control valve releases the treated melt after twin-screw high shear at an accurate temperature and a given time. From the schematics of the twin-screw device, it shows that the high shear stress is applied on the melt where the screws are in contact with each other and screw tip reaching to the barrel wall.

With the distinct advantage for viscous liquid applications, the twin-screw device is capable of being operated at temperatures above or below the liquidus of the liquid feed to provide treated liquid metal or highly sheared semi-solid slurry. Previous research showed that the well dispersed nano-size native MgO oxide films resulted in a refined microstructure, uniform distribution of solute elements through the enhanced heterogeneous nucleation [68]. Moreover, excellent dispersion of SiC particles from micron to nano scale has been obtained in Al metal matrix composites through the twin-screw based high shear treatment [67, 73].

3.2.2. Rotor-stator Mechanism High Shear Dispersion

High shear mixers, also known as high shear reactors, rotor-stator mixers, and high shear homogenizers have been widely used in chemical, pharmaceutical and food industries for emulsification, suspension and chemical reaction purpose [22]. They are characterised by high rotor tip speeds (10-50 m/s), high shear rate (10^4-10^5 s^{-1}) and highly localized energy dissipation rates near the mixing head.

The rotor-stator based high shear melt conditioning (HSMC) device developed within Brunel Centre for Advanced Solidification Technology (BCAST) provides intensive melt shearing, dispersing inclusions into finer scale particles that enhance the number of nucleation sites [64]. It is comprised of a set of rotor and stator attached to an electrical motor with a speed control. During its operation, the motor transfers the power to the rotor by the shaft and drives the rotor to spin and shear the melt in the gap between the rotor and the inside of the stator and also in the openings of the stator (Fig. **2**). The rotation speed can be in the order of 1,000-10,000 rpm providing an extremely high shear rate. Since the rotor is spinning at high speed, this creates a centrifugal force that displaces the melt upwards in a pumping action, followed by squeezing the same volume of melt through the stator holes. The HSMC technique provides macro-flow in a volume of melt for distributive mixing and intensive shearing near the tip of the device for dispersive mixing.

The main advantages include; significantly enhanced kinetics for chemical reactions or phase transformations, uniform dispersion, distribution and size reduction of solid particles and gas bubbles, improved homogenisation of chemical composition and temperature fields and also forced wetting of usually difficult-to-wet solid particles in the liquid metal. Hence, the HSMC technology can be used for: physical grain refinement by dispersing naturally occurring oxides [69], for degassing of melts [74], for the preparation of metal matrix (nano) composites [75, 76] and also for preparation of semi-solid slurries [66]. In turn, these characteristics can be applied to benefit various conventional casting processes, in order to improve the quality of cast products.

4. MAGNESIUM BASED MMNCS

Since HSDT could offer an ideal combination of refined microstructures and homogeneous spatial distribution of particles, many investigations have been made to fabricate metal matrix based nanocomposites (MMNCs), particularly on light metals, such as Mg alloys due to its high strength-to-weight ratio compared to other structural metals.

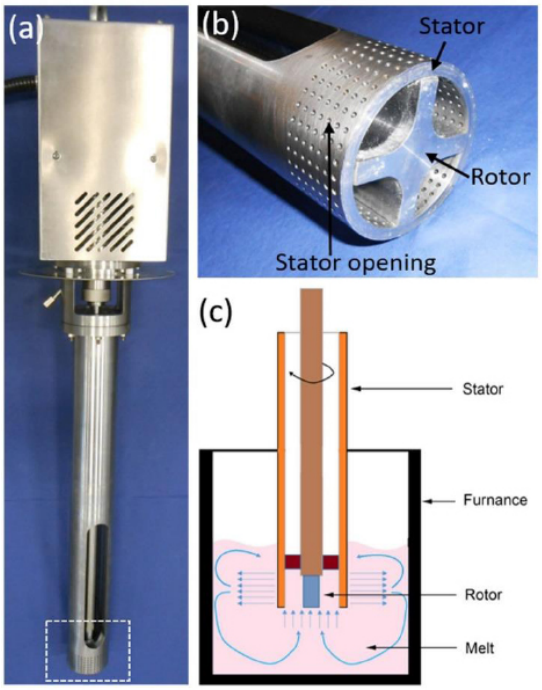

Fig. (2). (**a**) The mixer used for HSDT, (**b**) the stator, rotor and stator openings in the mixer and (**c**) schematic illustration of the high shearing process [2]. *(A higher resolution / colour version of this figure is available in the electronic copy of the article).*

The nanoparticles (NPs) usually incorporated in Mg alloys include but are not limited to ceramic reinforcements, such as Al_2O_3, AlN, SiC, Y_2O_3 *etc*. [18-79]. In order to combine the suitable mechanical properties with excellent corrosion resistance, many studies selected ceramic nanoparticles containing human bone compositions such as hydroxyapatite (HA), beta-tricalcium phosphate (β-TCP) and MgO, to fabrication MMNCs. In the following sections, the Mg based MMNCs will be reviewed according to different types of NPs incorporated by HSDT.

4.1. AlN

AlN NPs were considered as promising nucleation sites for Mg alloys due to their same hexagonal closed packed (hcp) structure with similar lattice parameters [80, 81]. Many efforts have been made to reveal the influence of AlN NPs on the creep resistance of Mg based MMNCs, Yang *et al.* [82] employed HSDT to fabricate the mixture of 0.75% AlN NPs and 0.25% metallic Al (AlN/Al, 80 nm) to Mg-2.85Nd-0.92Gd-0.41Zr-0.29Zn (El21) alloy. Shearing speed was fixed at 500 and 3000 rpm for 1 min. It was shown that the creep resistance of El21 was improved by approximately one order of magnitude with the addition of 0.5% AlN/Al NPs by HSDT at 3000 rpm, (Figs. **3a** and **b**). Moreover, El21 with 0.5% AlN/Al NPs showed even higher creep resistance with assistance of HSDT than that incorporated using US-assisted treatment with more addition (1%)

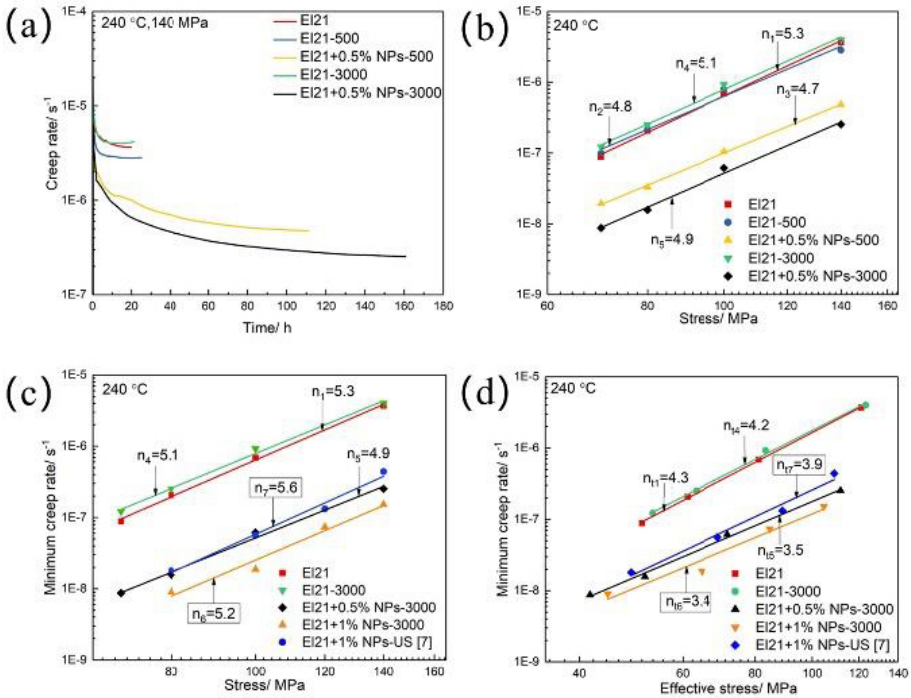

Fig. (3). (**a**) Creep rate as a function of creep time at 240°C for non-sheared El21, El21 sheared at 500 rpm, El21+0.5% AlN/Al sheared at 500 rpm, El21 sheared at 3000 rpm and El21+0.5% AlN/Al sheared at 3000 rpm, (**b**) minimum creep rate under different applied stress, (**c**) comparison of minimum creep rate of materials prepared using HSDT and US and (**d**) minimum creep rate as a function of effective stress [82]. *(A higher resolution / colour version of this figure is available in the electronic copy of the article).*

[78], which further indicated HSDT was more effective to disperse the NPs than the latter, (Fig. **3c** and **d**). They proposed that high speed turbulence generated from HSDT was helpful for promoting the physical contact between AlN NPs and matrix and increased their wetting, leading to a uniform distribution of AlN NPs. The addition of AlN/Al NPs in El21 by HSDT also led to a refined, thinner and homogeneous eutectic phase, which was beneficial for alleviating the grain boundary sliding and dislocation movement during creep.

Since the superiority of HSDT for the fabrication of Mg-based MMNCs was demonstrated in [82], further research was focused on the optimum content of AlN/Al on the improvement of creep resistance in El21 alloy [83]. 0, 0.25, 0.5 and 1% contents of AlN/Al NPs were added to El21 alloy using HSDT, respectively. The grains were coarsened by adding AlN/Al NPs due to the loss of grain refiner Zr for the formation of Al-Zr phase. Table **1** summarises the grain size and hardness of the nanocomposites with different contents of AlN/Al particles prepared at a shear speed of 3000 rpm and a duration of shearing of one minute.

Table 1. Grain size and hardness of AlN/Al-particle reinforced nanocomposites with Elektron21 matrix [83].

AlN/Al Content [wt.%]	Grain Size [μm]	Hardness [HV5]
0	80.1 ± 5.0	45.0 ± 1.2
0.25	86.4 ± 2.7	46.3 ± 2.6
0.5	144.5 ± 4.0	45.7 ± 2.4
1	463.5 ± 17.5	51.1 ± 3.6

Tension and compression tests at room temperature were carried out on the Elektron21 and the 0.5% NP nanocomposite [84]. Two different shear rates of 500 and 3000 rpm were used. Tables **2** and **3** show the results of the tests. It is clear that the room temperature properties cannot be improved by shearing and addition of NP. This is mainly due to the reduction of the grain refining effect of the Zr, which is inhibited by the addition of Al.

Table 2. Results of tensile tests at RT performed on Elektron21 as cast and sheared with 500 and 3000 rpm, and the 0.5AlN-nanocomposite [84].

Material	YS [MPa]	UTS [MPa]	E [%]
E21 as cast	102.3 ± 1.5	197.4 ± 4.2	10.1 ± 1.9
E21 500 rpm	94.0 ± 1.2	169.5 ± 12.9	6.9 ± 1.5
E21 3000 rpm	97.4 ± 2.2	189.1 ± 3.4	8.4 ± 1.1
E21+0.5AlN 500 rpm	92.1 ± 1.5	167.4 ± 10.1	5.8 ± 1.6
E21+0.5AlN 3000 rpm	95.4 ± 2.1	167.8 ± 2.3	5.9 ± 0.5

(YS: Yield Strength; UTS: Ultimate Tensile Strength; E: Elongation)

However, the intermetallic phase was sheared to be more homogeneous in the matrix with reduced size. Such phase and AlN NPs could act as reinforcements on the grain boundaries and matrix to enhance the creep resistance of El21, thus El21+1% AlN/Al showed the best creep resistance among all the materials.

Table 3. Results of tensile tests at RT performed on Elektron21 as cast and sheared with 500 and 3000 rpm, and the 0.5AlN-nanocomposite [84].

Material	CYS [MPa]	UCS [MPa]	C [%]
E21 as cast	113.3 ± 1.4	333.8 ± 1.4	16.4 ± 0
E21 500 rpm	103.4 ± 1.2	322.3 ± 0.9	17.7 ± 0.6
E21 3000 rpm	110.0 ± 0.7	330.0 ± 0.5	16.8 ± 1.3
E21+0.5AlN 500 rpm	98.5 ± 0.4	320.6 ± 1.5	19.4 ± 0.5
E21+0.5AlN 3000 rpm	102.8 ± 0.7	328.8 ± 2.0	17.0 ± 0.6

(CYS: Compressive Yield Strength; UCS: Ultimate Compressive Strength; C: Compression)

It is noticed that the aforementioned NPs contain 75% AlN and 25% Al. Therefore it is of interest to differentiate the individual/synergistic roles of AlN and Al NPs on the creep resistance of El21 by HSDT. Yang *et al.* [85] further compared the creep resistance of El21 alloy with additions of pure 0.25 Al%, 0.75% AlN and 1% AlN/Al NPs sheared by HSDT. They claimed that the simultaneous addition of Al and AlN NPs played a synergistic strengthening effect on the creep resistance of El21 alloy. HSDT was not only beneficial for dispersing the NPs uniformly in the matrix, but also promoted the chemical reactions between Al and RE for the formation of Al_2RE. Such structure was more thermally stable to inhibit the dislocation movement and transfer the load from matrix to NPs.

Since El21 alloy is a heat treatable alloy [86], Yang *et al.* [87] investigated the influence of T6 heat treatment on the creep resistance of El21+1% AlN/Al NPs stirred by HSDT. They found additional plate-like Al_2RE precipitates were formed after T6 heat treatment (green arrows in Fig. (**4f**), while there were no such precipitates in NP-free El21 alloy (Fig. **4c**). This formation of plate-like Al_2RE precipitates consumed certain amount of RE solutes and decreased the amount of γ" and β' precipitates in the subsequent ageing process. Therefore, they provided a reduced the precipitation strengthening during creep and were detrimental to the creep resistance of El21+1% AlN/Al (T6) MMNCs (Figs. **4a-f**).

4.2. Hydroxyapatite

Hydroxyapatite (HA) NPs have been extensively utilized for bone grafting and biomimetic coatings, which were capable of improving corrosion resistance and strength of materials [88]. This made them promising for tailoring both the corrosion resistance and mechanical properties simultaneously in Mg based MMNCs. Razavi *et al.* [89] fabricated an Mg-1.61Zn-0.18Mn-0.5Ca+1% HA (Compositions in wt.% throughout unless specified) nanocomposites by a novel route combining HSDT and equal channel angular extrusion (ECAE) technique, followed by heat treatment. It is found that the combination of HSDT and ECAE effectively decreased its biodegradation rate with a marginal corrosion rate of 0.12 mm/year. This is ascribed to the improvement of

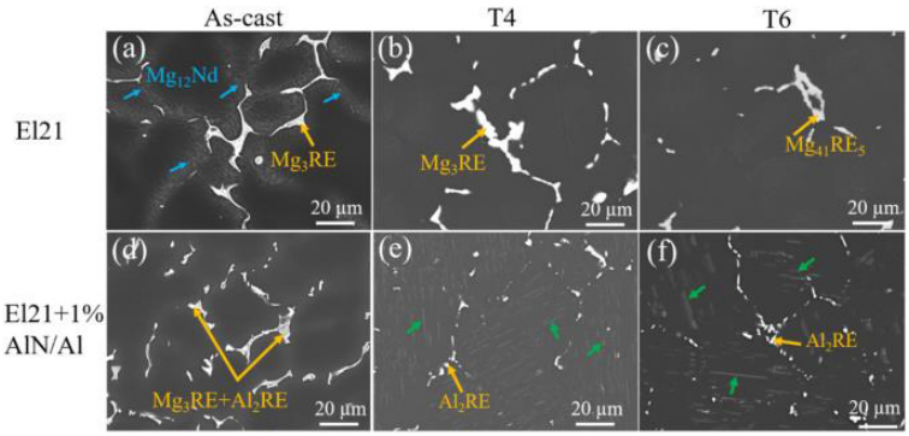

Fig. (4). (**a-f**) SEM micrographs of El21 and its nanocomposites in as-cast, T4 and T6-treated conditions [87]. *(A higher resolution / colour version of this figure is available in the electronic copy of the article).*

wettability between reinforcements and matrix with the assistance of HSDT and ECAE.

However, HSDT/ECAE showed diverse responses to corrosion resistance depending on the shapes of HA NPs. Razavi *et al.* [90] added two commercial available HA NPs as reinforcements to Mg-2Zn-0.2Mn-0.5Ca fabricated with HSDT and ECAE (Fig. **5a**), which have spherical and needle morphologies with an average size of 40 nm (Fig. **5b**). It was found that spherical HA NPs showed better corrosion resistance than needle morphology ones. This was attributed to the relatively worse wettability between needle HA NPs and matrix than that of spherical ones. It was more difficulty for needle HA NPs to physically contact with the alloy matrix due to their sharp corners, which made their bonding loose. Meanwhile, residual stress concentrations around the needle HA NPs were readily created, which might result in pitting corrosions and promote local corrosion.

Li *et al.* [88, 91] used HSDT to fabricate the Mg-3Zn-0.5Zr+HA NPs MMNCs followed by ECAE technique. Spherical HA NPs with an average size of 35 nm were selected as reinforcements at different amounts of weight percentage, *i.e.* 1, 3, 5 and 10 wt. %. The shearing speed of HSDT was controlled at several speeds up to 10000 rpm for 5-20 min. The optimum shearing speed was found to be approximately 5000 rpm for 10 min and holding for less than 3 min prior to solidification. Fig. (**6**) exhibited the comparisons of as cast microstructures of Mg-3Zn-0.5Zr+5% HA with and without high shearing. HSDT led to a refined microstructure with a uniform spatial dispersion of HA NPs (Fig. **6a**), while Fig. (**6b**) showed coarse grains and HA NPs aggregated randomly as large clusters in the matrix. They claimed that the grain size of high-sheared MMNCs was only about one tenth to that of non-sheared ones, which was distinctly smaller than those fabricated by PM process. HSDT enhanced the wettability between HA NPs and the matrix and effectively broke down the HA clusters in the molten metal, which led to an obvious improvement on the mechanical properties. It is shown that Mg-3Zn-0.5Zr with

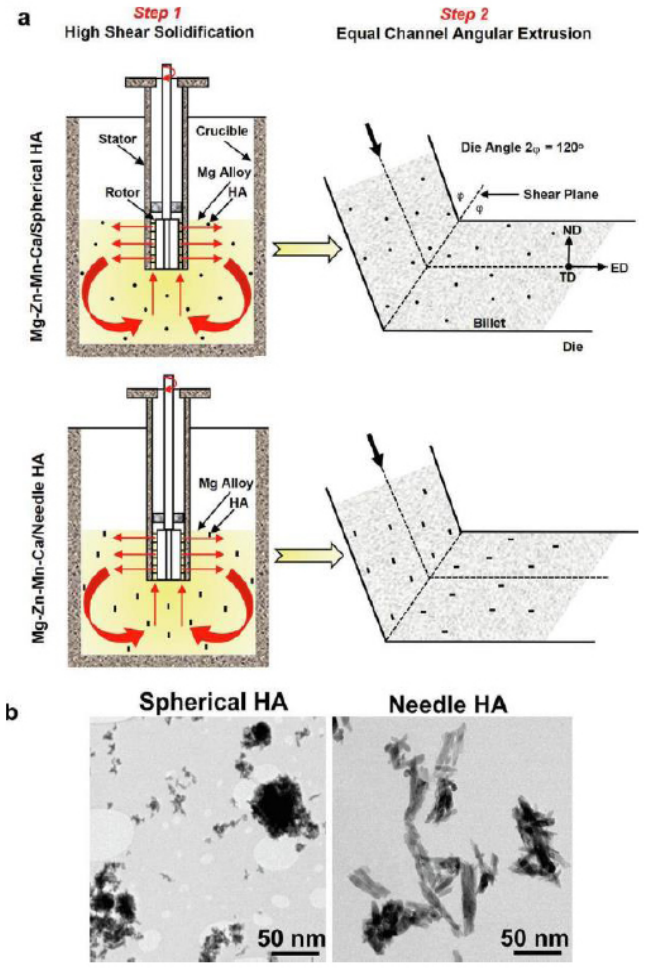

Fig. (5). (**a**) Schematic illustrations of the fabrication process with the combination of HSDT and ECAE for Mg-2Zn-0.2Mn-0.5-Ca+1% HA nanocomposites, (**b**) TEM micrographs of spherical and needle HA NPs [90]. *(A higher resolution / colour version of this figure is available in the electronic copy of the article).*

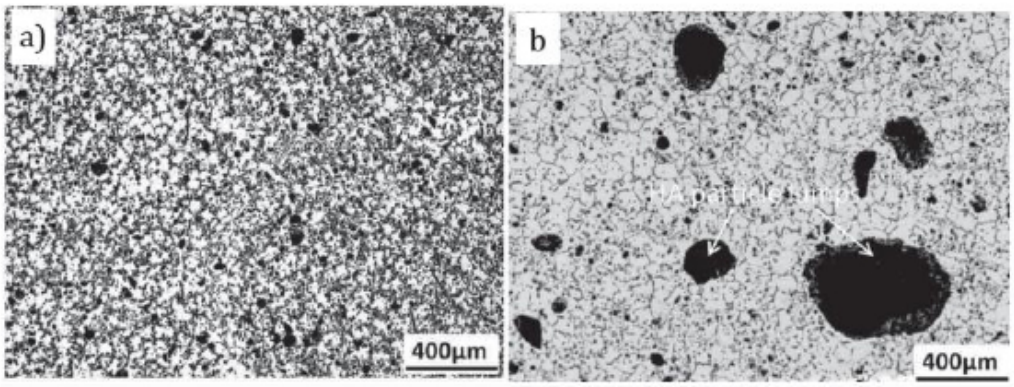

Fig. (6). Optical micrographs of as-cast Mg-3Zn-0.5Zr+5% HA NPs processed with high shearing (**a**) and without high shearing (**b**) [88].

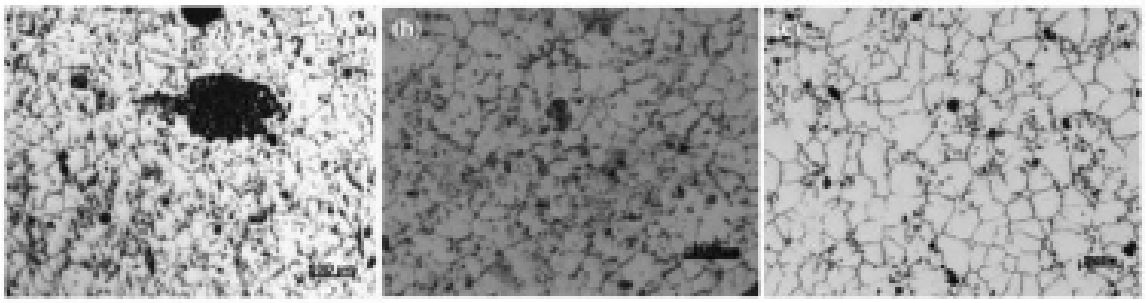

Fig. (7). Optical microstructures of Mg-3Zn-1Ca+1% β-TCP MMNCs after (**a**) conventional mechanical stirring, (**b**) HSDT and (**c**) HSDT+MCAST, respectively [76].

addition of 3-5% HA NPs showed a better combination of strength and ductility than those of commercial Mg wrought alloys.

4.3. β-TCP

TCP ($Ca_3(PO_4)_2$) NPs were capable of offering superior biocompatibility, bioactivity and osteoconductive performances, which make them possible as bone graft substitute. It is reported that $Ca_3(PO_4)_2$ group acted as the largest inorganic constituent in human bone tissue and had wide applications in orthopedic and dental usage [92, 93]. Meanwhile, compared with HA particles, TCP exhibits higher dissolution rate, which makes them promising as complete degradation implant materials. Liu *et al.* [76] employed HSDT to incorporate β-TCP NPs in Mg-3Zn-Ca matrix. Such β-TCP powder has spheroid-like morphology with a diameter of less than 100 nm. After adding 1% β-TCP NPs in the melt, the mixer of HSDT was controlled over a range of 6000-8000 rpm at 640°C melt temperature for 4-5 min before being subjected to another rheo-diecasting process (M-CAST) process [94]. Fig. (**7a**) exhibits severe agglomeration of β-TCP NPs located in the matrix after conventional stirring. After intensive shearing by HSDT, β-TCP clusters were homogeneously dispersed as smaller-sized ones (Fig. **7b**). With combination of HSDT and MCAST, the agglomeration of β-TCP NPs were further alleviated in Fig. (**7c**). They proposed that with the assistance of HSDT β-TCP NPs were effectively to break up and wet with Mg-3Zn-Ca matrix due to an extremely high shear area generated by HSDT.

Huang *et al.* [95] combined HSDT with ECAE process to fabricate a biodegradable Mg based MMNCs with β-TCP NPs. Its corrosion resistance was determined *via* electrochemical test. 1% β-TCP NPs with a diameter rang of 100-200 nm were incorporated by HSDT at a shearing speed of 1200 rpm for 5 min at 650°C prior to ECAE process. It is claimed that a refined uniform grain structure were obtained with the addition of β-TCP NPs after intensive shearing by HSDT. This was a result of HSDT providing an equilibrium temperature and uniform chemical compositions in the melt, which spread the nucleation agents homogeneously throughout the melt to make the most of their effects. Such microstructures given by HSDT and ECAE contributed to the improvement of both the hardness and corrosion resistance of Mg-2Zn-1Ca+1% β-TCP. Vickers-hardness values are given in Table **4**.

Table 4. Vickers micro-hardness of materials [95].

Process	As-cast	1ECAE	2ECAE	4ECAE
HV0.1	55.1 ± 3.7	72.4 ± 6.8	77.8 ± 2.4	80.6 ± 1.9

4.4. MgO

Previous studies reported that HA particles exhibited a poor interface with Mg matrix [96] and showed very low solubility *in vivo.* [97]. MgO particles were one of the important constituents in bioglass, which were bioactive, antibacterial and capable of full degradation. These advantages make them as one of the promising reinforcements for the fabrication of biomedical MMNCs.

Lin *et al.* [98] used MgO NPs with spherical morphology with an average diameter of 50-100 nm to reinforce the Mg-3Zn-0.2Ca matrix. Four different amounts of weight percentage, *i.e.* 0.1, 0.2, 0.3 and 0.5%, were incorporated by HSDT at a shearing speed of 4000 rpm for 5 min at 680°C before extrusion. The microstructural analysis showed that a relatively good dispersion of MgO particles were achieved by HSDT. A good interface between MgO NPs and matrix was observed where no cracks or voids were formed. Mg-3Zn-0.2Ca with 0.5% MgO NPs exhibited the best mechanical properties in terms of tensile yield stress and ultimate tensile stress. The refined grain size and good interface between MgO NPs and Mg matrix, which resulted from the assistance of HSDT, contributed to the improvement of corrosion resistance, Table **5**. Moreover, MgO was helpful for the generation of $Mg(OH)_2$ films in the early stage of immersion.

Table 5. Grain size and corrosion rate of materials [98].

Material	Grain Size [µm]		Corrosion Rate [mm/y]
-	As-cast	As-extr.	
MZC	90 ± 5	2 ± 0.5	6.44 ± 0.65
MZCs	125± 5	10 ± 0.8	4.45 ± 0.21
MZC0.1s	55 ± 4	5.1 ± 0.3	3.92 ± 0.45
MZC0.2s	50 ± 3	3.1 ± 0.4	3.10 ± 0.20
MZC0.3s	46 ± 3	2.2 ± 0.4	3.55 ± 0.42
MZC0.5s	37 ± 2	1.5 ± 0.2	5.40 ± 0.30

CONCLUSION

The following nanoparticles used as reinforcement materials in Mg based MMNCs were presented: AlN, HA, β-TCP and MgO. AlN nanoparticles in El21+1% AlN/Al NPs stirred by HSDT tended to form Al_2RE phase which has higher thermal stability than that of Mg_3RE thus improved creep resistance. Following HSDT, HA nanoparticles had greater wettability to the Mg matrix due to the breaking up of HA clusters. This led to an obvious improvement to mechanical properties. The intensive shearing by HSDT and ECAE contributed to the improvement of both the hardness and corrosion resistance of Mg-2Zn-1Ca+1% β-TCP as a result of the refinement of grain structures in β-TCP nanoparticles. Finally, MgO NPs, initially selected for their biocompatibility properties, were incorporated in Mg-3Zn-0.2Ca *via* HSDT. Good grain refinement was achieved which contributed to improve corrosion resistance and ultimately allowed MgO to generate $Mg(OH)_2$ films in early stages of immersion.

FUTURE OUTLOOK

In order to be able to dare an outlook into the future of magnesium-based nanocomposites, this hybrid material must certainly be investigated in more detail. The effect of various nanoparticles on the solidification behaviour of different magnesium melts is not yet fully understood, and the processes for their production can still be optimised. The *in-situ* production of the nanoparticles during a chemical reaction prior to solidification is another interesting way to control the quantity, size and distribution of the particles.

Functionalisation through incorporated nanoparticles is also conceivable in the future. This is possible, for example, in medical applications in which degradable magnesium implants release fluorescent nanoparticles during degradation, the detection of which in the blood can then provide information about the degradation rate of the implant. But also nanoparticles that lead to repeated grain refinement after melting of the nanocomposite and subsequent solidification are of interest. They can be used in powders or wires that are used in additive manufacturing. In the additively manufactured component, the fine-grained material has a strength and ductility advantage compared to conventional magnesium alloys.

AUTHORS' CONTRIBUTION

HY, JP, XY, SG, and HD contributed to collecting, writing, reviewing the text. HD contributed the idea for the review.

CONSENT FOR PUBLICATION

Not applicable.

FUNDING

None.

CONFLICT OF INTEREST

The authors declare no conflict of interest, financial or otherwise.

ACKNOWLEDGEMENTS

None.

REFERENCES

[1] Parande G, Manakari V, Kumar Meenashisundaram G, Gupta M. Enhancing the hardness/compression/damping response of magnesium by reinforcing with biocompatible silica nanoparticulates. Int J Mater Res 2016; 107(12): 1091-9. http://dx.doi.org/10.3139/146.111435

[2] Hassan SF, Gupta M. Development and characterization of ductile Mg/Y_2O_3 nanocomposites. J Eng Mater Technol 2007; 129(3): 462-7. http://dx.doi.org/10.1115/1.2744418

[3] Chen Y, Tekumalla S, Guo YB, Gupta M. Introducing Mg-4Zn-3Gd-1Ca/ZnO nanocomposite with compressive strengths matching/exceeding that of mild steel. Sci Rep 2016; 6: 32395. http://dx.doi.org/10.1038/srep32395 PMID: 27572903

[4] Paramsothy M, Chan J, Kwok R, Gupta M. Al_2O_3 nanoparticle addition to commercial magnesium alloys: multiple beneficial effects. Nanomaterials (Basel) 2012; 2(2): 147-62.

http://dx.doi.org/10.3390/nano2020147 PMID: 28348301
[5] Johanes M, Tekumalla S, Gupta M. Fe_3O_4 Nanoparticle-reinforced magnesium nanocomposites processed *via* disintegrated melt deposition and turning-induced deformation techniques. Metals (Basel) 2019; 9(11): 1225.
http://dx.doi.org/10.3390/met9111225
[6] Goh CS, Wei J, Lee LC, Gupta M. Simultaneous enhancement in strength and ductility by reinforcing magnesium with carbon nanotubes. Mater Sci Eng A 2006; 423(1-2): 153-6.
http://dx.doi.org/10.1016/j.msea.2005.10.071
[7] Azarniya A, Safavi MS, Sovizi S, *et al.* Metallurgical challenges in carbon nanotube-reinforced metal matrix nanocomposites. Metals (Basel) 2017; 7: 384.
http://dx.doi.org/10.3390/met7100384
[8] Xiang S, Wang X, Gupta M, Wu K, Hu X, Zheng M. Graphene nanoplatelets induced heterogeneous bimodal structural magnesium matrix composites with enhanced mechanical properties. Sci Rep 2016; 6: 38824.
http://dx.doi.org/10.1038/srep38824 PMID: 27941839
[9] Kandemir S. Development of graphene nanoplatelet-reinforced AZ91 magnesium alloy by solidification processing. JMEPEG 2018; 27: 3014-23.
http://dx.doi.org/10.1007/s11665-018-3391-x
[10] Chang YW, Pozuelo M, Yang JM. Thermally stable nanostructured magnesium nanocomposites reinforced by diamantane. JOM 2015; 67(12): 2828-33.
http://dx.doi.org/10.1007/s11837-015-1637-8
[11] Gong H, Anasori B, Dennison CR, *et al.* Fabrication, biodegradation behavior and cytotoxicity of Mg-nanodiamond composites for implant application. J Mater Sci Mater Med 2015; 26(2): 110.
http://dx.doi.org/10.1007/s10856-015-5441-3 PMID: 25665844
[12] Pozuelo M, Chang YW, Yang JM. Effect of diamondoids on the microstructure and mechanical behaviour of nanostructured Mg-matrix nanocomposites. Mater Sci Eng A 2015; 633: 200-8.
http://dx.doi.org/10.1016/j.msea.2015.02.062
[13] Dieringa H, Katsarou L, Buzolin R, *et al.* Ultrasound assisted casting of an AM60 based metal matrix nanocomposite, its properties, and recyclability. Metals (Basel) 2017; 7: 388.
http://dx.doi.org/10.3390/met7100388
[14] Sillekens WH, Jarvis DJ, Vorozhtsov A, *et al.* The ExoMet project: EU/ESA research on high-performance light-metal alloys and nanocomposites. Metal Mater Trans 2014; 45: 3349-61.
http://dx.doi.org/10.1007/s11661-014-2321-2
[15] Dieringa H. Processing of magnesium-based metal matrix nanocomposites by ultrasound-assisted particle dispersion: a review. Metals (Basel) 2018; 8: 431.
http://dx.doi.org/10.3390/met8060431
[16] Manoylov A, Bojarevics V, Pericleous K. Modeling the break-up of nano-particle clusters in aluminum- and magnesium-based metal matrix nano-composites. Metall Mater Trans, A Phys Metall Mater Sci 2015; 46: 2893-907.
http://dx.doi.org/10.1007/s11661-015-2934-0
[17] Kaldre I, Bojarevics A, Grants I, *et al.* Nanoparticle dispersion in liquid metals by electromagnetically induced acoustic cavitation. Acta Mater 2016; 118: 253-9.
http://dx.doi.org/10.1016/j.actamat.2016.07.045
[18] Dieringa H. Properties of magnesium alloys reinforced with nanoparticles and carbon nanotubes: a review. J Mater Sci 2011; 46: 289-306.
http://dx.doi.org/10.1007/s10853-010-5010-6
[19] Gupta M, Wong WLE. An introduction to lightweight, energy saving, environment friendly magnesium based nanocomposites: materials of upcoming generation. Adv Mat Res 2015; 1125: 3-7.
http://dx.doi.org/10.4028/www.scientific.net/AMR.1125.3
[20] Gupta M, Wong WLE. Magnesium-based nanocomposites: lightweight materials of the future. Mater Charact 2015; 105: 30-46.
http://dx.doi.org/10.1016/j.matchar.2015.04.015
[21] Jayakumar J, Raghunath BK, Rao TH. Recent development and challenges in synthesis of magnesium matrix nano composites- a review. Int J Lat Res Sci Techn 2012; 1(2): 164-71.
[22] Paul EL, Atiemo-Obeng VA, Kresta SM. Handbook of industrial mixing: science and practice. United States: John Wiley & Sons 2004.
[23] Benjamin JS. Dispersion strengthened superalloys by mechanical alloying. Metall Trans 1970; 1: 2943-51.
[24] Rawal SP. Metal-matrix composites for space applications. JOM 2001; 53: 14-7.
http://dx.doi.org/10.1007/s11837-001-0139-z
[25] Clyne T, Withers P. An introduction to metal matrix composites. Cambridge, UK: Cambridge University Press 1995.
[26] Chandrashekar A, Ajaykumar BS, Reddappa HN. Mechanical, structural and corrosion behaviour of AlMg4.5/nano Al_2O_3 metal matrix composites. Mater Tod Proc 2018; 5: 2811-7.
[27] Bhuiyan MMH, Wang J, Li LH, *et al.* Boron nitride nanotube reinforced titanium metal matrix composites with excellent high-temperature performance. J Mater Res 2017; 32: 3744-52.
http://dx.doi.org/10.1557/jmr.2017.345
[28] Yang Y, Lan J, Li X. Study on bulk aluminum matrix nano-composite fabricated by ultrasonic dispersion of nano-sized SiC particles in molten aluminum alloy. Mater Sci Eng A 2004; 380: 378-83.
http://dx.doi.org/10.1016/j.msea.2004.03.073
[29] Shi L, Sun C, Liu W. Electrodeposited nickel-cobalt composite coating containing MoS2. Appl Surf Sci 2008; 254: 6880-5.
http://dx.doi.org/10.1016/j.apsusc.2008.04.089
[30] Roy D, Singh S, Basu B, Lojkowski W, Mitra R, Manna I. Studies on wear behavior of nano-intermetallic reinforced Al-base amorphous/nanocrystalline matrix *in situ* composite. Wear 2009; 266: 1113-8.
http://dx.doi.org/10.1016/j.wear.2009.03.015
[31] Wang J, Li Z, Fan G, Pan H, Chen Z, Zhang D. Reinforcement with graphene nanosheets in aluminum matrix composites. Scr Mater 2012; 66: 594-7.
http://dx.doi.org/10.1016/j.scriptamat.2012.01.012
[32] Neubauer E, Kitzmantel M, Hulman M, Angerer P. Potential and challenges of metal-matrix-composites reinforced with carbon nanofibers and carbon nanotubes. Compos Sci Technol 2010; 70: 2228-36.
http://dx.doi.org/10.1016/j.compscitech.2010.09.003
[33] Lloyd D. Particle reinforced aluminium and magnesium matrix composites. Int Mater Rev 1994; 39: 1-23.
http://dx.doi.org/10.1179/imr.1994.39.1.1
[34] Harrigan WC Jr. Commercial processing of metal matrix composites. Mater Sci Eng A 1998; 244: 75-9.
http://dx.doi.org/10.1016/S0921-5093(97)00828-9
[35] Kainer KU. Metal matrix composites: custom-made materials for automotive and aerospace engineering. United State: John Wiley & Sons 2006.
http://dx.doi.org/10.1002/3527608117
[36] Attar H, Ehtemam-Haghighi S, Kent D, Dargusch MS. Recent developments and opportunities in additive manufacturing of titanium-based matrix composites: a review. Int J Mach Tools Manuf 2018; 133: 85-102.
http://dx.doi.org/10.1016/j.ijmachtools.2018.06.003
[37] Hashim J, Looney L, Hashmi M. Metal matrix composites: production by the stir casting method. J Mater Process Technol 1999; 92: 1-7.
http://dx.doi.org/10.1016/S0924-0136(99)00118-1
[38] Tomas J. Adhesion of ultrafine particles-a micromechanical approach. Chem Eng Sci 2007; 62: 1997-2010.
http://dx.doi.org/10.1016/j.ces.2006.12.055
[39] Israelachvili J, Tabor D. Van der Waals forces: theory and experiment. Prog Surf Memb Sci 1973; 7: 1-55.
http://dx.doi.org/10.1016/B978-0-12-571807-3.50006-5
[40] Rumpf H. Die Wissenschaft des Agglomerierens. Chemieingenieurtechnik (Weinh) 1974; 46: 1-11.
http://dx.doi.org/10.1002/cite.330460102
[41] Schubert H. Grundlagen des Agglomerierens. Chemieingenieurtechnik (Weinh) 1979; 51: 266-77.
http://dx.doi.org/10.1002/cite.330510404
[42] Tomas J, Schubert H. Modelling of the strength and the flow properties of moist soluble bulk materials. Aufbereit Tech 1982; 23: 507-15.
[43] Sukumaran K, Pillai S, Pillai R, *et al.* The effects of magnesium additions on the structure and properties of Al-7 Si-10 SiCp com-

posites. J Mater Sci 1995; 30: 1469-72.
http://dx.doi.org/10.1007/BF00375250
[44] Rohatgi P, Asthana R, Das S. Solidification, structures, and properties of cast metal-ceramic particle composites. Int Met Rev 1986; 31: 115-39.
[45] Wang Q, Callisti M, Miranda A, McKay B, Deligkiozi I, Milickovic TK, *et al.* Evolution of structural, mechanical and tribological properties of Ni-P/MWCNT coatings as a function of annealing temperature. Surf Coat Tech 2016; 302: 195-201.
http://dx.doi.org/10.1016/j.surfcoat.2016.06.011
[46] Miranda A, Alba-Baena N, McKay BJ, Eskin DG, Ko SH, Shin J. Study of mechanical properties of an LM24 composite alloy reinforced with Cu-CNT nanofillers, processed using ultrasonic cavitation. 2013; 765: 245-9.
http://dx.doi.org/10.4028/www.scientific.net/MSF.765.245
[47] Lloyd D, Jin I. A method of assessing the reactivity between SiC and molten AI. Metal Mater Trans 1988; 19: 3107-9.
http://dx.doi.org/10.1007/BF02647740
[48] Lloyd D. The solidification microstructure of particulate reinforced aluminium/SiC composites. Compos Sci Technol 1989; 35: 159-79.
http://dx.doi.org/10.1016/0266-3538(89)90093-6
[49] Redner S. Fragmentation. Statistical models for the fracture of disordered media 1990; 321-48.
[50] Cheng Z, Redner S. Kinetics of fragmentation. J Phys Math Gen 1990; 23: 1233.
http://dx.doi.org/10.1088/0305-4470/23/7/028
[51] Hansen S, Khakhar D, Ottino J. Dispersion of solids in nonhomogeneous viscous flows. Chem Eng Sci 1998; 53: 1803-17.
http://dx.doi.org/10.1016/S0009-2509(98)00010-4
[52] Rwei S, Manas-Zloczower I, Feke D. Observation of carbon black agglomerate dispersion in simple shear flows. Polym Eng Sci 1990; 30: 701-6.
http://dx.doi.org/10.1002/pen.760301202
[53] Stone HA. Dynamics of drop deformation and breakup in viscous fluids. Annu Rev Fluid Mech 1994; 26: 65-102.
http://dx.doi.org/10.1146/annurev.fl.26.010194.000433
[54] Rumpf H. The strength of granules and agglomerates. Agglomeration. New York, U.S.A.: Wiley 1962; pp. 379-418.
[55] Yang X, Barekar NS, Ji S, Dhindaw BK, Fan Z. Influence of reinforcing particle distribution on the casting characteristics of Al-SiCp composites. J Mater Process Technol 2020; 279: 116580.
http://dx.doi.org/10.1016/j.jmatprotec.2019.116580
[56] Kendall K. Agglomerate strength. Powder Metall 1988; 31: 28-31.
[57] Barailler F, Heniche M, Tanguy PA. CFD analysis of a rotor-stator mixer with viscous fluids. Chem Eng Sci 2006; 61: 2888-94.
http://dx.doi.org/10.1016/j.ces.2005.10.064
[58] Utomo A, Baker M, Pacek A. The effect of stator geometry on the flow pattern and energy dissipation rate in a rotor-stator mixer. Chem Eng Res Des 2009; 87: 533-42.
http://dx.doi.org/10.1016/j.cherd.2008.12.011
[59] Douglas JF, Gasiorek JM, Swaffield JA, Jack LB. Fluid mechanics. (6th ed..), Essex: Pearson Education Limited 2011.
[60] Hanumanth G, Irons G. Particle incorporation by melt stirring for the production of metal-matrix composites. J Mater Sci 1993; 28: 2459-65.
http://dx.doi.org/10.1007/BF01151680
[61] Afshar S, Allaire C. The corrosion of refractories by molten aluminum. JOM 1996; 48: 23-7.
http://dx.doi.org/10.1007/BF03222938
[62] Yan M, Fan Z. Review durability of materials in molten aluminum alloys. J Mater Sci 2001; 36: 285-95.
http://dx.doi.org/10.1023/A:1004843621542
[63] Mihelich J, Decker RF. Apparatus for processing corrosive molten metals. US Patent 5711366A, 1998.
[64] Fan Z, Jiang B, Zuo Y. Apparatus and method for liquid metals treatment. US Patent 9498820B2, 2016.
[65] Fan Z, Bevis MJ, Ji S. Method and apparatus for producing semi-solid method slurries and shaped components. US Patent 6745818B1, 2004.
[66] Patel JB, Yang X, Mendis CL, Fan Z. Melt conditioning of light metals by application of high shear for improved microstructure and defect control. JOM (1989) 2017; 69(6): 1071-6.
http://dx.doi.org/10.1007/s11837-017-2335-5 PMID: 32025178
[67] Hari Babu N, Tzamtzis S, Barekar N, Patel J, Fan Z. Fabrication of metal matrix composites under intensive shearing. 2008; 141: 373-8.
http://dx.doi.org/10.4028/3-908451-59-0.373
[68] Fan Z, Wang Y, Xia M, Arumuganathar S. Enhanced heterogeneous nucleation in AZ91D alloy by intensive melt shearing. Acta Mater 2009; 57: 4891-901.
http://dx.doi.org/10.1016/j.actamat.2009.06.052
[69] Li H, Wang Y, Fan Z. Mechanisms of enhanced heterogeneous nucleation during solidification in binary Al-Mg alloys. Acta Mater 2012; 60: 1528-37.
http://dx.doi.org/10.1016/j.actamat.2011.11.044
[70] Edwards MF, Baker MR. A review of liquid mixing equipment. In: Harnby N, Edwards MF, Nienow AW, Eds. Mixing in the process industries. (2nd ed.). Oxford: Butterworth-Heinemann 1992; pp. 118-36.
http://dx.doi.org/10.1016/B978-075063760-2/50028-7
[71] Tang H, Wrobel LC, Fan Z. Numerical evaluation of immiscible metallic Zn-Pb binary alloys in shear-induced turbulent flow. Mater Sci Eng A 2004; 365: 325-9.
http://dx.doi.org/10.1016/j.msea.2003.09.059
[72] Fan Z, Xia M, Zhang H, *et al.* Melt conditioning by advanced shear technology (MCAST) for refining solidification microstructures. Int J Cast Met Res 2009; 22: 103-7.
http://dx.doi.org/10.1179/136404609X367443
[73] Tzamtzis S, Barekar N, Babu NH, Patel J, Dhindaw B, Fan Z. Processing of advanced Al/SiC particulate metal matrix composites under intensive shearing-A novel Rheo-process. Compos Part A Appl Sci Manuf 2009; 40: 144-51.
http://dx.doi.org/10.1016/j.compositesa.2008.10.017
[74] Zuo Y, Jiang B, Zhang Y, Fan Z. Degassing LM25 aluminium alloy by novel degassing technology with intensive melt shearing. Int J Cast Met Res 2013; 26: 16-21.
http://dx.doi.org/10.1179/1743133612Y.0000000019
[75] Yang X, Huang Y, Barekar NS, Das S, Stone IC, Fan Z. High shear dispersion technology prior to twin roll casting for high performance magnesium/SiCp metal matrix composite strip fabrication. Compos Part A Appl Sci Manuf 2016; 90: 349-58.
http://dx.doi.org/10.1016/j.compositesa.2016.07.025
[76] Liu D, Zuo Y, Meng W, Chen M, Fan Z. Fabrication of biodegradable nano-sized β-TCP/Mg composite by a novel melt shearing technology. Mater Sci Eng C 2012; 32: 1253-8.
http://dx.doi.org/10.1016/j.msec.2012.03.017
[77] Dieringa H, Huang Y, Maier P, Hort N, Kainer KU. Tensile and compressive creep behaviour of Al_2O_3(Saffil) short fiber reinforced magnesium alloy AE42. Mater Sci Eng A 2005; 410: 85-8.
http://dx.doi.org/10.1016/j.msea.2005.08.005
[78] Katsarou L, Mounib M, Lefebvre W, *et al.* Microstructure, mechanical properties and creep of magnesium alloy Elektron21 reinforced with AlN nanoparticles by ultrasound-assisted stirring. Mater Sci Eng A 2016; 659: 84-92.
http://dx.doi.org/10.1016/j.msea.2016.02.042
[79] Jie C, Bao C, Chen F. Evolutions of microstructure and mechanical properties for Mg-Al/AlN composites under hot extrusion. Mater Sci Eng A 2016; 667: 426-34.
http://dx.doi.org/10.1016/j.msea.2016.05.033
[80] Chen J, Bao CG, Wang Y, Liu JL, Suryanarayana C. Microstructure and lattice parameters of aln particle-reinforced magnesium matrix composites fabricated by powder metallurgy. Acta Metall Sin 2015; 28(1): 1354-63.
http://dx.doi.org/10.1007/s40195-015-0333-6
[81] Fu HM, Zhang MX, Qiu D, Kelly PM, Taylor JA. Grain refinement by AlN particles in Mg-Al based alloys. J Alloys Compd 2009; 478: 809-12.
http://dx.doi.org/10.1016/j.jallcom.2008.12.029
[82] Yang H, Huang Y, Song B, Kainer KU, Dieringa H. Enhancing the creep resistance of AlN/Al nanoparticles reinforced Mg-2.85Nd-0.92Gd-0.41Zr-0.29Zn alloy by a high shear dispersion technique. Mater Sci Eng A 2019; 755: 18-27.
http://dx.doi.org/10.1016/j.msea.2019.03.131
[83] Yang H, Huang Y, Gavras S, Kainer KU, Hort N, Dieringa H. Influences of AlN/Al nanoparticles on the creep properties of elek-

tron21 prepared by high shear dispersion technology. JOM 2019; 71(7): 2245-52.
http://dx.doi.org/10.1007/s11837-019-03499-4

[84] Yang H, Huang Y, Song B, Kainer KU, Hort N, Dieringa H. Microstructure, Mechanical and Creep Properties of Elektron21 Reinforced with AlN Nanoparticles by Intensive Melt Shearing. In: Fan Z, Mendis M, Eds. Proceedings of the 11th International Conference on Magnesium Alloys and their Application. 9781908549372-35.

[85] Yang H, Zander D, Huang Y, Kainer KU, Dieringa H. Individual/synergistic effects of Al and AlN on the microstructural evolution and creep resistance of Elektron21 alloy. Mat Sci Engin A 2020; 777: 139072.

[86] Kielbus A. Microstructure and mechanical properties of Elektron 21 alloy after heat treatment. J Achievem Mat Manuf Engin 2007; 20: 127-30.

[87] Yang H, Zander D, Jiang B, *et al.* Effects of heat treatment on the microstructural evolution and creep resistance of Elektron21 alloy and its nanocomposite. Mater Sci Eng A 2020; 789: 139669.
http://dx.doi.org/10.1016/j.msea.2020.139669

[88] Huang Y, Li J, Zhou L. Mg-3Zn-0.5Zr/HA nanocomposites fabricated by high shear solidification and equal channel angular extrusion. Mater Sci Technol 2018; 34: 1868-79.
http://dx.doi.org/10.1080/02670836.2018.1495880

[89] Razavi M, Huang Y. A Magnesium-based nanobiocomposite processed by a novel technique combining high shear solidification and hot extrusion. Recent Pat Nanotechnol 2019; 13(1): 38-48.
http://dx.doi.org/10.2174/1872210513666181231122808 PMID: 30599113

[90] Razavi M, Huang Y. Effect of hydroxyapatite (HA) nanoparticles shape on biodegradation of Mg/HA nanocomposites processed by high shear solidification/equal channel angular extrusion route. Mater Lett 2020; 267: 127541.
http://dx.doi.org/10.1016/j.matlet.2020.127541

[91] Li J, Huang Y. Microstructure and mechanical properties of an Mg-3Zn-0.5Zr-5HA nanocomposite processed by ECAE. IOP Conf Series Mater Sci Eng 2014; 63: 012112.
http://dx.doi.org/10.1088/1757-899X/63/1/012112

[92] Ryu HS, Youn HJ, Hong KS, Chang BS, Lee CK, Chung SS. An improvement in sintering property of beta-tricalcium phosphate by addition of calcium pyrophosphate. Biomaterials 2002; 23(3): 909-14.
http://dx.doi.org/10.1016/S0142-9612(01)00201-0 PMID: 11771710

[93] Ryu HS, Hong KS, Lee JK, *et al.* Magnesia-doped HA/β-TCP ceramics and evaluation of their biocompatibility. Biomaterials 2004; 25(3): 393-401.
http://dx.doi.org/10.1016/S0142-9612(03)00538-6 PMID: 14585687

[94] Fan Z. Development of the rheo-diecasting process for magnesium alloys. Mater Sci Eng A 2005; 413-414: 72-8.
http://dx.doi.org/10.1016/j.msea.2005.09.038

[95] Huang Y, Liu DB, Xia MX, Anguiliano L. Characterization of an Mg-2Zn-1Ca 1β-TCP composite fabricated by high shear solidification and ECAE. Mater Sci Forum 2013; 765: 813-7.
http://dx.doi.org/10.4028/www.scientific.net/MSF.765.813

[96] Gu X, Zhou W, Zheng Y, Dong L, Xi Y, Chai D. Microstructure, mechanical property, bio-corrosion and cytotoxicity evaluations of Mg/HA composites. Mater Sci Eng C 2010; 30: 827-32.
http://dx.doi.org/10.1016/j.msec.2010.03.016

[97] Kwon SH, Jun YK, Hong SH, Kim HE. Synthesis and dissolution behavior of β-TCP and HA/β-TCP composite powders. J Eur Ceram Soc 2003; 23: 1039-45.
http://dx.doi.org/10.1016/S0955-2219(02)00263-7

[98] Lin G, Liu D, Chen M, *et al.* Preparation and characterization of biodegradable Mg-Zn-Ca/MgO nanocomposites for biomedical applications. Mater Charact 2018; 144: 120-30.
http://dx.doi.org/10.1016/j.matchar.2018.06.028